

CERN-TH.7430/94

Towards a Model Independent Analysis of Rare B Decays

Ahmed Ali, Gian Giudice and Thomas Mannel
Theory Division, CERN, CH-1211 Geneva 23, Switzerland

We propose to undertake a model-independent analysis of the inclusive decay rates and distributions in the processes $B \rightarrow X_s \gamma$ and $B \rightarrow X_s \ell^+ \ell^-$ ($B = B^\pm$ or B_d^0). We show how measurements of the decay rates and distributions in these processes would allow us to extract the magnitude and sign of the dominant Wilson coefficients of the magnetic moment operator $m_b \bar{s}_L \sigma_{\mu\nu} b_R F^{\mu\nu}$ and the four-fermion operators $(\bar{s}_L \gamma_\mu b_L)(\bar{\ell} \gamma^\mu \ell)$ and $(\bar{s}_L \gamma_\mu b_L)(\bar{\ell} \gamma^\mu \gamma^5 \ell)$.

Contribution to the
27th International Conference on High Energy Physics
 Glasgow, Scotland, 20 – 27 July 1994

Towards a Model Independent Analysis of Rare B Decays

Ahmed Ali^{‡¶}, Gian Giudice^{§†} and Thomas Mannel^{||}

Theory Division, CERN, CH-1211 Geneva 23, Switzerland.

Abstract

We propose to undertake a model-independent analysis of the inclusive decay rates and distributions in the processes $B \rightarrow X_s \gamma$ and $B \rightarrow X_s \ell^+ \ell^-$ ($B = B^\pm$ or B_d^0). We show how measurements of the decay rates and distributions in these processes would allow us to extract the magnitude and sign of the dominant Wilson coefficients of the magnetic moment operator $m_b \bar{s}_L \sigma_{\mu\nu} b_R F^{\mu\nu}$ and the four-fermion operators $(\bar{s}_L \gamma_\mu b_L)(\bar{\ell} \gamma^\mu \ell)$ and $(\bar{s}_L \gamma_\mu b_L)(\bar{\ell} \gamma^\mu \gamma^5 \ell)$.

1. The Decay $B \rightarrow X_s \gamma$ in SM and Experiment

The measurements of the decay mode $B \rightarrow K^* \gamma$, reported last year by the CLEO collaboration [1], having a branching ratio $\mathcal{B}(B \rightarrow K^* \gamma) = (4.5 \pm 1.0 \pm 0.9) \times 10^{-5}$, and the inclusive decay $B \rightarrow X_s \gamma$, reported at this conference [2] with a branching ratio $\mathcal{B}(B \rightarrow X_s \gamma) = (2.32 \pm 0.51 \pm 0.32 \pm 0.20) \times 10^{-4}$, have put the physics of the electromagnetic penguins on an experimental footing. In the standard model (SM), these transitions are dominated by the short-distance contributions and provide valuable information about the top quark mass and the Cabibbo-Kobayashi-Maskawa (CKM) weak mixing matrix elements $V_{ts} V_{tb}$ [3]. The rapport between the SM and experiment may be quantified in terms of the CKM matrix element ratio [4]:

$$0.62 \leq \left| \frac{V_{ts}}{V_{cb}} \right| \leq 1.1, \quad (1)$$

which is consistent with unity, resulting from the unitarity constraints. Alternatively, one can set $V_{ts}/V_{cb} = 1$ to obtain from the CLEO measurement bounds on the Wilson coefficient $C_7(m_b)$ of the effective

magnetic moment operator. Using $\mathcal{B}(B \rightarrow X_s \gamma)$ from [2], one obtains

$$0.22 \leq |C_7(m_b)| \leq 0.30. \quad (2)$$

Using, however, the 90%-confidence-level range from the CLEO measurement $\mathcal{B}(B \rightarrow X_s \gamma) = (2.31 \pm 1.1) \times 10^{-4}$ and the theoretical calculation for $\mathcal{B}(B \rightarrow X_s \gamma)$ from [4] we obtain

$$0.19 \leq |C_7(m_b)| \leq 0.32. \quad (3)$$

We also remark that the photon energy and hadron mass spectra measured by CLEO are in good agreement with the SM-based calculations in [5]. The bound (2) can be used to constrain the non-SM contribution to the decay rate $\mathcal{B}(B \rightarrow X_s \gamma)$ as discussed in these proceedings [6, 7].

2. Motivation for a Model Independent Analysis of Rare B Decays

The determination of $|C_7(m_b)|$ from the inclusive branching ratio $\mathcal{B}(B \rightarrow X_s \gamma)$ is a prototype of the kind of analysis that we would like to propose here to be carried out for the rare B decays in general and for the semileptonic decays $B \rightarrow X_s \ell^+ \ell^-$, in particular. First steps towards a model-independent analysis of the FCNC electroweak rare B decays involving these decay modes have recently been proposed in [8], to which we refer for details and references to other related work. Here, we summarize the main assumptions and results.

‡ e-mail: alia@cernvm.cern.ch

¶ On leave of absence from DESY, Hamburg, FRG.

§ e-mail: giudice@vxcern.cern.ch

† On leave of absence from INFN, Sezione de Padova, Italy.

|| e-mail: mannel@cernvm.cern.ch

The main interest in rare B decays is to measure the effective FCNC vertices in order to test the SM and search for new physics. We have argued that with some plausible assumptions these vertices can be parametrized through a limited number of effective parameters, which govern the rates and shapes (differential distributions) in rare B decays $B \rightarrow X_s \gamma$, $B \rightarrow X_s \ell^+ \ell^-$ and $B_s \rightarrow \ell^+ \ell^-$. The search for physics beyond the SM in these decays can be carried out in terms of three effective parameters, $C_7(\mu)$, $C_9(\mu)$ and $C_{10}(\mu)$, characterizing the strength of the magnetic moment and two four-fermion operators $(\bar{s}_L \gamma_\mu b_L)(\ell \gamma^\mu \ell)$ and $(\bar{s}_L \gamma_\mu b_L)(\bar{\ell} \gamma^\mu \gamma^5 \ell)$. This can then be interpreted in a large class of models. The presence of non-SM physics may manifest itself by distorting the differential distributions in $B \rightarrow X_s \ell^+ \ell^-$. Some possible examples of such distortions have been worked out in [8]. Here we present profiles of the Wilson coefficients in the best-motivated extensions of the SM, namely the Minimal Supersymmetric Standard Model (MSSM).

Our analysis is based on an effective Hamiltonian of the form

$$\mathcal{H}_{eff}(b \rightarrow sX) = -\frac{4G_F}{\sqrt{2}} \lambda_t \sum_{i=1}^{10} C_i(\mu) \mathcal{O}_i(\mu). \quad (4)$$

where X stands for $q\bar{q}$, γ , gluon and $\ell^+ \ell^-$ and $\lambda_t = V_{ts}^* V_{tb}$. The operator basis $\mathcal{O}_{1\dots 10}$ is given in [8] and is the same as in the SM, thereby restricting our analysis to cases, in which the effective Hamiltonian may be written as (4).

3. Analysis of the Decays $B \rightarrow X_s \gamma$ and $B \rightarrow X_s \ell^+ \ell^-$

The experimental quantities we consider in this paper are the following: (i) **Inclusive radiative rare decay branching ratio** $\mathcal{B}(B \rightarrow X_s \gamma)$; (ii) **Invariant dilepton mass distributions** in $B \rightarrow X_s \ell^+ \ell^-$; (iii) **Forward-backward (FB) charge asymmetry** $\mathcal{A}(\hat{s})$ in $B \rightarrow X_s \ell^+ \ell^-$.

The FB asymmetry $\mathcal{A}(\hat{s})$ is defined with respect to the angular variable $z \equiv \cos \theta$, where θ is the angle of the ℓ^+ with respect to the b -quark direction in the centre-of-mass system of the dilepton pair. It is obtained by integrating the doubly differential distribution $d^2\mathcal{B}/(dz d\hat{s})(B \rightarrow X_s \ell^+ \ell^-)$ [9]:

$$\mathcal{A}(\hat{s}) \equiv \int_0^1 dz \frac{d^2\mathcal{B}}{dz d\hat{s}} - \int_{-1}^0 dz \frac{d^2\mathcal{B}}{dz d\hat{s}}, \quad (5)$$

where $\hat{s} = (p_1 + p_2)^2/m_b^2$ and p_1 and p_2 denote, respectively, the momenta of the ℓ^+ and ℓ^- .

We remark that the decay rate $\mathcal{B}(B \rightarrow X_s \gamma)$ puts a bound on the absolute value of the coefficient $C_7(\mu)$.

However, the radiative B decay rate by itself is not able to distinguish between the solutions $C_7(\mu) > 0$ (holding in the SM) and the solutions $C_7(\mu) < 0$, which, for example, are also allowed in the MSSM as one scans over the allowed parameter space. We recall that the invariant dilepton mass distribution and the forward-backward asymmetry in $B \rightarrow X_s \ell^+ \ell^-$ are sensitive to the sign and magnitude of $C_7(\mu)$ [9]. Using \mathcal{H}_{eff} given in (4), one obtains for the dilepton invariant mass distribution

$$\begin{aligned} \frac{d\mathcal{B}}{d\hat{s}} &= \mathcal{B}_{sl} \frac{\alpha^2}{4\pi^2} \frac{\lambda_t}{|V_{cb}|} \frac{\hat{w}(\hat{s})}{f(m_c/m_b)} & (6) \\ &\times \left[(|C_9 + Y(\hat{s})|^2 + C_{10}^2) \alpha_1(\hat{s}, \hat{m}_s) \right. \\ &\left. + \frac{4}{\hat{s}} C_7^2 \alpha_2(\hat{s}, \hat{m}_s) + 12\alpha_3(\hat{s}, \hat{m}_s) C_7 (C_9 + \operatorname{Re} Y(\hat{s})) \right], \end{aligned}$$

where the auxiliary functions α_i depend only on the kinematic variables and $Y(\hat{s})$ depends on the coefficients C_1, \dots, C_6 of the four quark operators (see [8]).

The corresponding differential asymmetry as defined in (5) is

$$\begin{aligned} \mathcal{A}(\hat{s}) &= -\mathcal{B}_{sl} \frac{3\alpha^2}{8\pi^2} \frac{1}{f(m_c/m_b)} \hat{w}^2(\hat{s}) C_{10} & (7) \\ &\times [\hat{s}(C_9 + \operatorname{Re} Y(\hat{s})) + 4C_7(1 + \hat{m}_s^2)]. \end{aligned}$$

We first present the partial branching ratio $\mathcal{B}(\Delta s)$ and partial FB asymmetry $\mathcal{A}(\Delta s)$, where Δs defines an interval in the dilepton invariant mass. In order to minimize long-distance effects we shall consider the kinematic regime for s below the J/ψ mass (low invariant mass) and for s above the mass of the ψ' (high invariant mass). Integrating (7) over these regions for the invariant mass one finds

$$\mathcal{B}(\Delta s) = A(\Delta s) (C_9^2 + C_{10}^2) + B(\Delta s) C_9 + C(\Delta s), \quad (8)$$

where A , B and C are fixed in terms of the Wilson coefficients $C_1 \dots C_6$ and C_7 . For the numerical analysis we use $m_b = 4.7$ GeV, $m_c = 1.5$ GeV, $m_s = 0.5$ GeV. The resulting coefficients A , B , and C are listed in Table 1 for the decays $B \rightarrow X_s e^+ e^-$ and $B \rightarrow X_s \mu^+ \mu^-$.

For a measured branching fraction $\mathcal{B}(\Delta s)$, one can solve the above equation for $\mathcal{B}(\Delta s)$, obtaining a circle in the C_9 - C_{10} plane, with centre lying at $C_9^* = B(\Delta s)/(2A(\Delta s))$ and $C_{10}^* = 0$. The radius of this circle is proportional to $\sqrt{\mathcal{B}(\Delta s) - \mathcal{B}_{min}(\Delta s)}$, where the minimum branching fraction

$$\mathcal{B}_{min}(\Delta s) = C(\Delta s) - \frac{B^2(\Delta s)}{4A(\Delta s)} \quad (9)$$

is determined mainly by the present data on $B \rightarrow X_s \gamma$, i.e. by $|C_7|$.

Δs	C_7	$A(\Delta s)$	$B(\Delta s)$	$C(\Delta s)$ $\ell = e$	$C(\Delta s)$ $\ell = \mu$
$4m_\ell^2 < s < m_{J/\psi}^2$	+0.3	2.86	-5.76	84.1	76.6
$4m_\ell^2 < s < m_{J/\psi}^2$	-0.3	2.86	-20.8	124	116
$m_{\psi'}^2 < s < (1 - m_s^2)$	+0.3	0.224	-0.715	0.654	0.654
$m_{\psi'}^2 < s < (1 - m_s^2)$	-0.3	0.224	-1.34	2.32	2.32

Table 1. Values for the coefficients $A(\Delta s)$, $B(\Delta s)$ and $C(\Delta s)$ (in units of 10^{-8}) for the decay $B \rightarrow X_s \ell^+ \ell^-$.

Δs	C_7	$\alpha(\Delta s)$	$\beta(\Delta s)$
$4m_\ell^2 < s < m_{J/\psi}^2$	+0.3	-6.08	-24.0
$4m_\ell^2 < s < m_{J/\psi}^2$	-0.3	-6.08	55.4
$m_{\psi'}^2 < s < (1 - m_s^2)$	+0.3	-0.391	0.276
$m_{\psi'}^2 < s < (1 - m_s^2)$	-0.3	-0.391	1.37

Table 2. Values for the coefficients $\alpha(\Delta s)$ and $\beta(\Delta s)$ (in units of 10^{-9}).

To further pin down the Wilson coefficients, one could perform a measurement of the forward-backward asymmetry \mathcal{A} . Integrating (5) over a range (Δs) yields

$$\mathcal{A}(\Delta s) = C_{10} (\alpha(\Delta s) C_9 + \beta(\Delta s)). \quad (10)$$

For a fixed value of $\mathcal{A}(\Delta s)$, one obtains hyperbolic curves in the C_9 - C_{10} plane; like the coefficients A , B and C , the parameters α and β are given in terms of the Wilson coefficients $C_1 \cdots C_6$, C_7 and Δs ; their values are presented in Table 2.

Given the two experimental inputs, the branching fraction $\mathcal{B}(\Delta s)$ and the corresponding asymmetry $\mathcal{A}(\Delta s)$, one obtains a fourth-order equation for the Wilson coefficients C_9 and C_{10} , which admits in general four solutions, which can be plotted as contours for a fixed value for the branching fraction $\mathcal{B}(\Delta s)$ and the FB asymmetry $\mathcal{A}(\Delta s)$. The possible solutions for C_9 and C_{10} are given by the intersections of the circle corresponding to the measured branching fraction and the hyperbola, corresponding to the measured asymmetry. Details can be seen in [8].

We stress that the spectrum itself is very sensitive to the values of the Wilson coefficients and to the sign of C_7 . In fig. 1 we plot the various contributions to the spectrum, for positive and for negative C_7 .

In a similar way, it may become possible to measure also the differential asymmetry (5); the various contributions to $\mathcal{A}(s)$ are shown in fig. 2.

4. Model Predictions for the Wilson Coefficients

As an illustrative example we shall consider here the MSSM; we shall show, how the predictions for the

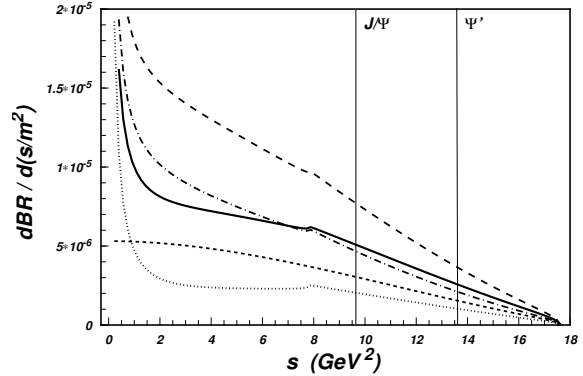


Figure 1. The dependence of the invariant-mass spectrum on the Wilson coefficients. Solid line: SM. Long-dashed line: $C_7 \rightarrow -C_7$, with other coefficients retaining their SM values. Short-dashed line: The contribution of C_{10} only. Dotted line: $C_{10} = 0$, with other coefficients retaining their SM values. Dash-dotted line: same as for the dotted one, but with $C_7 = -0.3$. The vertical lines indicate the location of the J/Ψ and Ψ' resonances.

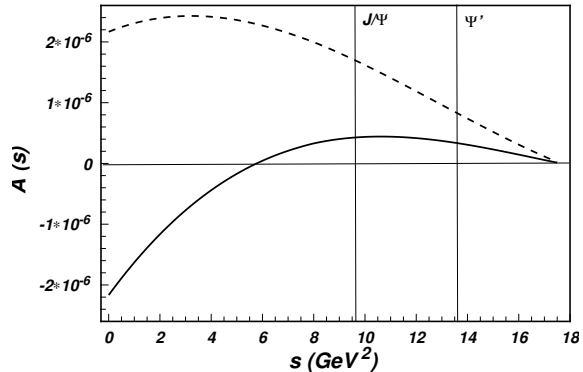


Figure 2. The dependence of the differential FB asymmetry on the Wilson coefficients. Solid line: SM. Long-dashed line: $C_7 \rightarrow -C_7$, with the other parameters retaining their SM values. The vertical lines indicate the location of the J/Ψ and Ψ' resonances.

Wilson coefficients C_7 , C_9 , and C_{10} are altered in this model.

Once the gluino contributions (as well as the analogous ones from neutralino exchange) are neglected, the flavour violation in the supersymmetric models is completely specified by the familiar CKM matrix. The one-loop supersymmetric corrections to the Wilson coefficients C_7 , C_9 , and C_{10} are given by two classes of diagrams: charged-Higgs exchange and chargino exchange [10].

The charged-Higgs contribution is specified by two input parameters: the charged-Higgs mass (m_{H^+}) and the ratio of Higgs vacuum expectation values ($v_2/v_1 \equiv \tan \beta$). This contribution alone corresponds to the two-Higgs doublet model which has also been considered in [8].

In addition to the diagrams with charged-Higgs

exchange, the MSSM leads also to chargino-mediated diagrams. The chargino contribution is specified by six parameters. Three of them enter the 2×2 chargino mass matrix:

$$m_{\chi^+} = \begin{pmatrix} M & m_W \sqrt{2} \sin \beta \\ m_W \sqrt{2} \cos \beta & \mu \end{pmatrix}. \quad (11)$$

Following standard notations, we call $\tan \beta$ the ratio of vacuum expectation values, the same that appears also in the charged-Higgs sector, and M, μ the gaugino and higgsino mass parameters, subject to the constraint that the lightest chargino mass satisfies the LEP bound, $m_{\chi^+}^+ > 45$ GeV. The squark masses

$$m_{\tilde{q}^\pm}^2 = \tilde{m}^2 + m_q^2 \pm A \tilde{m} m_q \quad (12)$$

contain two additional free parameters besides the known mass of the corresponding quark m_q : a common supersymmetry-breaking mass \tilde{m} and the coefficient A . The last parameter included in our analysis is a common mass $m_{\tilde{l}}$ for sleptons, all taken to be degenerate in mass, with the constraint $m_{\tilde{l}} > 45$ GeV. Therefore the version of the MSSM we are considering is defined in terms of seven free parameters.

We have computed the Wilson coefficients in the MSSM and then varied the seven above-defined parameters in the experimentally allowed region. The results of our analysis are presented in fig. 3, which shows the regions of the $C_9 - C_{10}$ plane allowed by possible choices of the MSSM parameters. The upper plot of fig. 3 corresponds to parameters which give rise to positive (same sign as in the SM) values of C_7 , consistent with experimental results on $b \rightarrow s\gamma$ ($0.19 < C_7 < 0.32$), while the lower plot corresponds to values of C_7 with opposite sign ($-0.32 < C_7 < -0.19$). We also show how our results are affected by an improvement in the experimental limits on supersymmetric particle masses, as can be expected from the Tevatron and LEP 200. Fig. 3 also shows the $C_9 - C_{10}$ regions allowed by the MSSM if the further constraints $m_{H^+} > 150$ GeV, $m_{\tilde{t}}, m_{\chi^+}, m_{\tilde{l}} > 100$ GeV are imposed.

The regions shown in fig. 3 illustrate the typical trend of the supersymmetric corrections. If supersymmetric particles exist at low energies, we can expect larger values of C_{10} and smaller (negative) values of C_9 than those predicted by the SM. This is the general feature, although the exact boundaries of the allowed regions depend on the particular model-dependent assumptions one prefers to use. However, the most interesting feature of supersymmetry is that solutions with negative values of C_7 are possible and are still consistent with present data. Moreover, values of the other two coefficients C_9 and C_{10} sufficiently different from the SM are allowed, leading to measurable differences in the decay rates and distributions of $B \rightarrow X_s \ell^+ \ell^-$ and $B_s \rightarrow \ell^+ \ell^-$.

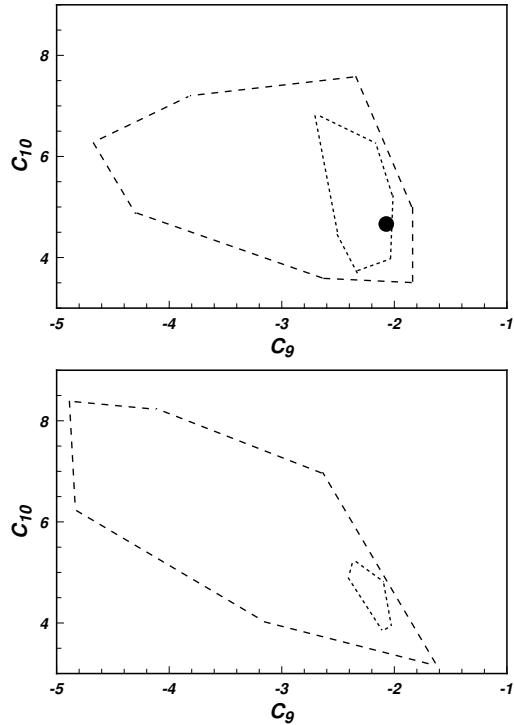


Figure 3. The region in the $C_9 - C_{10}$ plane obtained by varying the MSSM parameters. The upper (lower) plot corresponds to solutions that satisfy the $b \rightarrow s\gamma$ experimental constraint with positive (negative) C_7 given in eq.(2) and the present bounds ($m_{H^+} > 80$ GeV, $\tilde{m}_t, m_{\chi^+}, \tilde{m}_\ell > 45$ GeV). The smaller areas limited by the short-dashed line correspond to the region of the MSSM parameter space that will survive an unsuccessful search for supersymmetry at the Tevatron and LEP 200 ($m_{H^+} > 150$ GeV, $m_{\tilde{t}}, m_{\chi^+}, m_{\tilde{l}} > 100$ GeV).

References

- [1] R. Ammar et al. (CLEO Collaboration), Phys. Rev. Lett. **71** (1993) 674.
- [2] E. Thorndike (CLEO Collaboration), these proceedings.
- [3] N. Cabibbo, Phys. Rev. Lett. **10** (1963) 531; M. Kobayashi and T. Maskawa, Prog. Theor. Phys. **49** (1973) 652.
- [4] A. Ali and C. Greub, Z. Phys. **C60** (1993) 433.
- [5] A. Ali and C. Greub, Z. Phys. **C49** (1991) 431; Phys. Lett. **259B** (1991) 182.
- [6] N. G. Deshpande, these proceedings.
- [7] P. Nath, these proceedings.
- [8] A. Ali, G. Giudice and T. Mannel, CERN-TH.7346/94.
- [9] A. Ali, T. Mannel and T. Morozumi, Phys. Lett. **B273** (1991) 505; B. Grinstein, M.J. Savage and M.B. Wise, Nucl. Phys. **B319** (1989) 271; W. Jaus and D. Wyler, Phys. Rev. **D41** (1990) 3405; D. Wyler (private communication).
- [10] S. Bertolini, F. Borzumati, A. Masiero, and G. Ridolfi, Nucl. Phys. **B353** (1991) 591.